Available online at www.sciencedirect.com

ScienceDirect

Procedia Engineering 14 (2011) 3095–3103

Procedia Engineering

www.elsevier.com/locate/procedia

The Twelfth East Asia-Pacific Conference on Structural Engineering and Construction

A Substructuring Method for Model Updating and Damage Identification

Yong Xia*, Shun Weng, and You-Lin Xu

Department of Civil and Structural Engineering, The Hong Kong Polytechnic University

Abstract

Model updating of large-scale structures is time-consuming as the global system matrices need to be assembled continuously and the global eigensolutions and eigensensitivities are required in each iteration, even only a few elemental parameters need updating. In this paper, a substructuring approach is proposed to extract the substructural dynamic flexibility matrices from the measured modal properties of the global structure under the constraints of force compatibility and displacement compatibility. Thereafter the focused substructure is treated as an independent structure and updated directly using the traditional model updating method. It not only reduces the size of the analytical model involved in model updating but also decreases the uncertain parameters that need updating, thus resulting in a rapid convergence of the optimization process. Moreover, if a particular substructure needs updating, the measurement can be focused on the local area of the interested substructure only and the requirement of measurement on the entire structure is avoided. A laboratory tested frame structure is employed to illustrate the effectiveness and accuracy of the proposed method.

KEYWORDS: Substructuring method; model updating; damage identification; modal flexibility; large-scale structures

* Corresponding author, E-mail: ceyxia@polyu.edu.hk

doi:10.1016/j.proeng.2011.07.389

1. INTRODUCTION

Model updating methods are widely employed to develop a more accurate finite element (FE) model in presenting the real structure for the usage of optimization design, damage identification, structural control, and structural health monitoring. The basic procedure of model updating is to continuously adjust the elemental parameters (usually stiffness properties) so that the model predictions agree with the measurements as closely as possible (Brownjohn 2007). Nevertheless, the conventional model updating procedure is usually expensive for a large-scale numerical model in terms of computation time and computer memory. For example, Xia et al. (2008) carried out a model updating exercise for the Balla Balla Bridge in Western Australia, which was modeled by 907 elements, 949 nodes, and 5,400 degrees of freedom (DOFs). Convergence of the optimization took 155 iterations and cost about 420 hours. Within each iteration, calculating the eigensolutions took about 10 seconds, whereas calculating the eigensensitivities with respect to the uncertain parameters took more than two hours. In another study, a fine FE model was established for Tsing Ma Suspension Bridge that consists of about 300,000 nodes, 450,000 elements and 1.2 million DOFs (Duan et al. 2006). It took about 5 hours to obtain the first 100 natural frequencies and mode shapes in a 64-bit Itanium server with 8 CPUs of 1.5 GHz each. Model updating is nearly impossible even in such an advanced computer. The considerable burden associated with the model updating method is due to two reasons: 1) the large-scale model is represented by large-size system matrices, and the repeated analysis of the large-size matrices is a heavy workload. 2) Many uncertain parameters need to be adjusted in a large-scale numerical model, which makes convergence of the large-scale optimization problem much more difficult. The substructuring method (Lallemand et al. 1999, Koh et al. 2003) has been found a promising solution for reducing computation load in engineering applications. In conventional substructuring approaches (Klerk et al. 2008, Weng, et al. 2009, Xia et al. 2010), the substructural eigensolutions and their derivatives of the independent substructures are assembled to recover the eigensolutions and eigensensitivities of the global structure. The eigenproperties of the global structure are then compared with those measured through the model updating procedure. Even though only a few elemental parameters need updating, the global system matrices need to be assembled and the global eigensolutions and eigensensitivities are required in each iteration.

This paper proposes a substructuring based model updating technique in which only one or more substructures need to be adjusted. First, the measured global modal data are disassembled to the substructure level. If the particular substructures need updating, only the substructures need to be measured in the experiment, thus avoiding the requirement of measurement of the entire structure. Second, the substructures are treated as independent structures and can be updated with the conventional model updating approach to reproduce the extracted substructural flexibility matrices. As only one substructure instead of the global structure is involved in model updating, computational work of optimization is reduced. Moreover, the number of updating parameters in the substructure is much less than that of the global structure, which further benefits the convergence of the optimization. Finally, a laboratory tested frame structure is employed to illustrate the effectiveness and accuracy of the proposed method.

2. EXTRACTION OF SUBSTRUCTURAL FLEXIBILITY

Let $\{x_g\}$ denote the nodal displacement vector and $\{f_g\}$ the external force vector of the global structure with N DOFs. The global structure comprises NS substructures. If the jth substructure (j=1, 2, …, NS) with $N^{(j)}$ DOFs has the nodal displacement vector $\{x^{(j)}\}$, force vector $\{f^{(j)}\}$, stiffness matrix $\mathbf{K}^{(j)}$ and flexibility matrix $\mathbf{F}^{(j)}$, the primitive forms of the substructural displacements, forces, stiffness and flexibility matrices are assembled as

$$\left\{x^p\right\} = \begin{Bmatrix} \left\{x^{(1)}\right\} \\ \vdots \\ \left\{x^{(j)}\right\} \\ \vdots \\ \left\{x^{(NS)}\right\} \end{Bmatrix},\ \left\{f^p\right\} = \begin{Bmatrix} \left\{f^{(1)}\right\} \\ \vdots \\ \left\{f^{(j)}\right\} \\ \vdots \\ \left\{f^{(NS)}\right\} \end{Bmatrix},\ \mathbf{K}^p = \begin{bmatrix} \mathbf{K}^{(1)} & & & & \\ & \ddots & & & \\ & & \mathbf{K}^{(j)} & & \\ & & & \ddots & \\ & & & & \mathbf{K}^{(NS)} \end{bmatrix},$$

$$\mathbf{F}^p = \begin{bmatrix} \mathbf{F}^{(1)} & & & & \\ & \ddots & & & \\ & & \mathbf{F}^{(j)} & & \\ & & & \ddots & \\ & & & & \mathbf{F}^{(NS)} \end{bmatrix} \tag{1}$$

Hereinafter, subscript 'g' denotes the variables of the original global structure, and superscript 'p' denotes the primitive assembly of the substructural variables. The primitive vectors and matrices take the size of $NP\times 1$ and $NP\times NP$, respectively, which is larger than that of the global structure of N. The primitive vectors or matrices are associated with the global ones by

$$\left\{x^p\right\} = \mathbf{L}^p\left\{x_g\right\},\ \left[\mathbf{L}^p\right]^T\left\{f^p\right\} = \left\{f_g\right\} \tag{2}$$

$$\left(\left[\mathbf{L}^p\right]^T\mathbf{K}^p\mathbf{L}^p\right)\left\{x_g\right\} = \left[\mathbf{L}^p\right]^T\mathbf{K}^p\left\{x^p\right\} = \left[\mathbf{L}^p\right]^T\left\{f^p\right\} = \left\{f_g\right\} = \mathbf{K}_g\left\{x_g\right\},\ \left[\mathbf{L}^p\right]^T\mathbf{K}^p\mathbf{L}^p = \mathbf{K}_g \tag{3}$$

where $\mathbf{L}^p$ is the geometric operator with a size of $NP\times N$ and is determined by the geometric relation between the substructures and the global structure. For example, if the jth DOF of the global structure corresponds to the ith DOF in the separated substructures, then $\mathbf{L}^p_{ij} = 1$.

The displacement of a substructure can be written as a superposition of its deformational and rigid body motions. Accordingly, the primitive substructural displacement vector can be written as

$$\left\{x^p\right\} = \mathbf{F}^p\left\{f^p\right\} + \mathbf{R}^p\left\{\alpha^p\right\} \tag{4}$$

where $\mathbf{R}^p$ is the diagonal assembly of the orthogonal rigid body modes of the independent substructures, and $\left\{\alpha^p\right\}$ acts as the modal participation factors of the substructural rigid body modes. Theoretically, if the jth substructure is free after partition, the flexibility matrix of the jth substructure does not exist. The flexibility matrix mentioned in this paper is regarded as the modal flexibility, which is contributed by the deformational motions and does not include those contributed by the rigid body motions.

To be an independent structure, the forces imposed on a substructure comprise the external force and the connecting force from the adjacent substructures. i.e.,

$$\left\{f^p\right\} = \left(\left[\mathbf{L}^p\right]^T\right)^+\left\{f_g\right\} + \mathbf{C}\left\{\tau\right\} = \left\{\tilde{f}_g\right\} + \mathbf{C}\left\{\tau\right\} \tag{5}$$

where the Lagrange multiplier $\{\tau\}$ represents the connecting force along the boundaries of the substructures. $\{\tilde{f}_g\} = \left(\left[\mathbf{L}^p\right]^T\right)^+ \{f_g\} = \tilde{\mathbf{L}}^p \{f_g\}$, $\tilde{\mathbf{L}}^p = \left(\left[\mathbf{L}^p\right]^T\right)^+$ is the generalized inverse of $\left[\mathbf{L}^p\right]^T$ and matrix $\mathbf{C}$ implicitly defines the general connection between the adjacent substructures.
Substitution of Eq. (5) into Eq. (4) gives

$$\{x^p\} = \mathbf{F}^p \{f^p\} + \mathbf{R}^p \{\alpha^p\} = \mathbf{F}^p \left(\{\tilde{f}_g\} + \mathbf{C}\{\tau\}\right) + \mathbf{R}^p \{\alpha^p\} \tag{6}$$

As for Eq. (2), the global displacement can be expressed by the substructural variables as

$$\{x_g\} = \left[\mathbf{L}^p\right]^+ \{x^p\} = \left[\tilde{\mathbf{L}}^p\right]^T \mathbf{F}^p \left(\{\tilde{f}_g\} + \mathbf{C}\{\tau\}\right) + \left[\tilde{\mathbf{L}}^p\right]^T \mathbf{R}^p \{\alpha^p\} \tag{7}$$

If the two variables $\{\tau\}$ and $\{\alpha^p\}$ are known, the global displacement $\{x_g\}$ and the external force $\{f_g\}$ can be related by the substructural flexibility matrix $\mathbf{F}^p$, taking the place of the global flexibility matrix $\mathbf{F}_g$. The two variables will be solved by considering the following two compatibility constraints.
The rigid body modes and the forces in the substructures satisfy the force equilibrium compatibility (Alvin and Park 1999)

$$\left[\mathbf{R}^p\right]^T \{f^p\} = \{\mathbf{0}\} \tag{8}$$

From the physical point of view, the null-space of matrix $\mathbf{C}$ bears the displacement compatibility (Weng et al. 2009)

$$\mathbf{C}^T \{x^p\} = \{\mathbf{0}\} \tag{9}$$

Substituting Eq. (5) and Eq. (6) into the above two compatibility equations

$$\left[\mathbf{R}^p\right]^T \left(\{\tilde{f}_g\} + \mathbf{C}\{\tau\}\right) = 0, \; \mathbf{C}^T \left(\mathbf{F}^p \left(\{\tilde{f}_g\} + \mathbf{C}\{\tau\}\right) + \mathbf{R}^p \{\alpha^p\}\right) = \{\mathbf{0}\} \tag{10}$$

Eq. (10) leads to the following coupled equation in terms of the variables $\{\tau\}$ and $\{\alpha^p\}$

$$\begin{bmatrix} \mathbf{F}_C & \mathbf{R}_C \\ \mathbf{R}_C^T & \mathbf{0} \end{bmatrix} \begin{Bmatrix} \tau \\ \alpha^p \end{Bmatrix} = \begin{Bmatrix} \mathbf{C}^T \mathbf{F}^p \tilde{f}_g \\ \left[\mathbf{R}^p\right]^T \tilde{f}_g \end{Bmatrix} \tag{11}$$

where $\mathbf{F}_C = \mathbf{C}^T \mathbf{F}^p \mathbf{C}$, $\mathbf{R}_C = \mathbf{C}^T \mathbf{R}^p$. Based on Eq. (11), the two variables are solved as

$$\{\alpha^p\} = \mathbf{K}_R^{-1} \left(\left[\mathbf{R}^p\right]^T - \mathbf{R}_C^T \mathbf{F}_C^{-1} \mathbf{C}^T \mathbf{F}^p\right) \{\tilde{f}_g\}, \; \{\tau\} = -\mathbf{F}_C^{-1} \mathbf{C}^T \mathbf{F}^p \{\tilde{f}_g\} + \mathbf{F}_C^{-1} \mathbf{R}_C \mathbf{K}_R^{-1} \left(\mathbf{R}_C^T \mathbf{F}_C^{-1} \mathbf{C}^T \mathbf{F}^p - \mathbf{R}^T\right) \{\tilde{f}_g\} \tag{12}$$

where $\mathbf{K}_R = \mathbf{R}_C^T \mathbf{F}_C^{-1} \mathbf{R}_C$.
As long as $\{\tau\}$ and $\{\alpha^p\}$ are solved, Eq. (7) is expressed as

$$\{x_g\} = \left[\tilde{\mathbf{L}}^p\right]^T \left(\mathbf{F}^p - \mathbf{F}^p \mathbf{K}_C \mathbf{F}^p + \mathbf{F}^p \mathbf{K}_C \mathbf{F}_R \mathbf{K}_C \mathbf{F}^p - \mathbf{F}^p \mathbf{K}_C \mathbf{F}_R - \mathbf{F}_R \mathbf{K}_C \mathbf{F}^p - \mathbf{F}^p \mathbf{H} \mathbf{F}^p + \mathbf{F}_R\right) \{\tilde{f}_g\}$$

$$= \left[\tilde{\mathbf{L}}^p\right]^T \left(\mathbf{F}^p - \mathbf{F}^p \mathbf{H} \mathbf{F}^p - \mathbf{F}^p \mathbf{K}_C \mathbf{F}_R - \mathbf{F}_R^T \mathbf{K}_C^T \mathbf{F}^p + \mathbf{F}_R\right) \tilde{\mathbf{L}}^p \{f_g\} \tag{13}$$

where $\mathbf{H}=\mathbf{K}_C-\mathbf{K}_C\mathbf{F}_R\mathbf{K}_C$, $\mathbf{K}_C=\mathbf{C}\mathbf{F}_C^{-1}\mathbf{C}^T$, $\mathbf{F}_R=\mathbf{R}^p\left(\left[\mathbf{R}^p\right]^T\mathbf{K}_C\mathbf{R}^p\right)^{-1}\left[\mathbf{R}^p\right]^T$.

In consequence, the global flexibility is related to the substructural flexibility by

$$\mathbf{L}^p\mathbf{F}_g\left[\mathbf{L}^p\right]^T=\mathbf{F}^p-\mathbf{F}^p\mathbf{K}_C\mathbf{F}_R-\mathbf{F}_R^T\mathbf{K}_C^T\mathbf{F}^p-\mathbf{F}^p\mathbf{H}\mathbf{F}^p+\mathbf{F}_R \tag{14}$$

Usually, it is difficult to measure the target structure at all DOFs, and it is necessary to reduce the full model to the desired DOFs. The force compatibility and the displacement compatibility in Eq. (10) are disassembled according to the master DOFs and the slave DOFs as

$$\begin{bmatrix}\mathbf{R}_a^p\\ \mathbf{R}_b^p\end{bmatrix}^T\left(\begin{Bmatrix}\{\tilde{f}_g\}_a\\ \{\tilde{f}_g\}_b\end{Bmatrix}+\begin{bmatrix}\mathbf{C}_a\\ \mathbf{C}_b\end{bmatrix}\{\tau\}\right)=\mathbf{0},\ \begin{bmatrix}\mathbf{C}_a\\ \mathbf{C}_b\end{bmatrix}^T\left(\begin{bmatrix}\mathbf{F}_{aa}^p & \mathbf{F}_{ab}^p\\ \mathbf{F}_{ba}^p & \mathbf{F}_{bb}^p\end{bmatrix}\left(\begin{Bmatrix}\{\tilde{f}_g\}_a\\ \{\tilde{f}_g\}_b\end{Bmatrix}+\begin{bmatrix}\mathbf{C}_a\\ \mathbf{C}_b\end{bmatrix}\{\tau\}\right)+\begin{bmatrix}\mathbf{R}_a^p\\ \mathbf{R}_b^p\end{bmatrix}\{\alpha^p\}\right)=\mathbf{0} \tag{15}$$

and the global displacement is expressed according to the master and slave DOFs as

$$\begin{Bmatrix}\{x_g\}_a\\ \{x_g\}_b\end{Bmatrix}=\begin{bmatrix}\tilde{\mathbf{L}}_{aa}^p & \\ & \tilde{\mathbf{L}}_{bb}^p\end{bmatrix}^T\begin{bmatrix}\mathbf{F}_{aa}^p & \mathbf{F}_{ab}^p\\ \mathbf{F}_{ba}^p & \mathbf{F}_{bb}^p\end{bmatrix}\left(\begin{Bmatrix}\{\tilde{f}_g\}_a\\ \{\tilde{f}_g\}_b\end{Bmatrix}+\begin{bmatrix}\mathbf{C}_a\\ \mathbf{C}_b\end{bmatrix}\{\tau\}\right)+\begin{bmatrix}\tilde{\mathbf{L}}_{aa}^p & \\ & \tilde{\mathbf{L}}_{bb}^p\end{bmatrix}^T\begin{bmatrix}\mathbf{R}_a^p\\ \mathbf{R}_b^p\end{bmatrix}\{\alpha^p\} \tag{16}$$

where the subscript 'a' represents the rows or columns corresponding to the master DOFs which are usually the measured DOFs in practice, and the subscript 'b' represents those of the slave DOFs. Similar to the aforementioned procedure for full-DOF model, the displacement vector of the global structure at the master DOFs can be expressed by the external forces as

$$\begin{aligned}\{x_g\}_a=\ &\left[\tilde{\mathbf{L}}_{aa}^p\right]^T\Big(\mathbf{F}_{aa}^p-\mathbf{F}_{aa}^p\mathbf{K}_{Ca}\mathbf{F}_{aa}^p+\mathbf{F}_{aa}^p\mathbf{K}_{Ca}\mathbf{F}_{Ra}\mathbf{K}_{Ca}\mathbf{F}_{aa}^p-\mathbf{F}_{aa}^p\mathbf{K}_{Ca}\mathbf{R}_a\mathbf{K}_{Ra}^{-1}\left[\mathbf{R}_a^p\right]^T\\ &-\mathbf{R}_a^p\mathbf{K}_{Ra}^{-1}\left[\mathbf{R}_a^p\right]^T\mathbf{K}_{Ca}\mathbf{F}_{aa}^p+\mathbf{R}_a^p\mathbf{K}_{Ra}^{-1}\left[\mathbf{R}_a^p\right]^T\Big)\tilde{\mathbf{L}}_{aa}^p\{f_g\}_a\end{aligned} \tag{17}$$

Finally, the substructural flexibility and global flexibility at the master DOFs are related by

$$\mathbf{L}_{aa}^p\left(\mathbf{F}_g\right)_{aa}\left[\mathbf{L}_{aa}^p\right]^T=\mathbf{F}_{aa}^p-\mathbf{F}_{aa}^p\mathbf{H}_{aa}\mathbf{F}_{aa}^p-\mathbf{F}_{aa}^p\mathbf{K}_{Ca}\mathbf{F}_{Ra}-\mathbf{F}_{Ra}\mathbf{K}_{Ca}\mathbf{F}_{aa}^p+\mathbf{F}_{Ra} \tag{18}$$

where $\mathbf{F}_{Ra}=\mathbf{R}_a\mathbf{K}_{Ra}^{-1}\left[\mathbf{R}_a^p\right]^T$, $\mathbf{H}_{aa}=\mathbf{K}_{Ca}-\mathbf{K}_{Ca}\mathbf{F}_{Ra}\mathbf{K}_{Ca}$. $\mathbf{F}_{Ca}=\mathbf{C}_a^T\mathbf{F}_{aa}\mathbf{C}_a$, $\mathbf{K}_{Ca}=\mathbf{C}_a\mathbf{F}_{Ca}^{-1}\mathbf{C}_a^T$, and $\mathbf{K}_{Ra}=\left[\mathbf{R}_a^p\right]^T\mathbf{K}_{Ca}\mathbf{R}_a^p=\left[\mathbf{R}_a^p\right]^T\mathbf{C}_a\mathbf{F}_{Ca}^{-1}\mathbf{C}_a^T\mathbf{R}_a^p$.

In Eq. (14) and Eq. (18), the substructural flexibility matrix $\mathbf{F}^p$ contributes to the global flexibility matrix $\mathbf{F}_g$ in a complicated manner. It is difficult to express $\mathbf{F}^p$ using the global flexibility $\mathbf{F}_g$ in an explicit form. An iterative scheme is deserved to obtain the substructural flexibility matrix $\mathbf{F}^p$, and the kth iteration is proceeded as

$$\left[\mathbf{F}_{aa}^p\right]^{[k]}=\left(\overline{\mathbf{F}}_g\right)_{aa}^E+\left[\mathbf{F}_{aa}^p\right]^{[k-1]}\mathbf{H}_{aa}^{[k-1]}\left[\mathbf{F}_{aa}^p\right]^{[k-1]}+\left[\mathbf{F}_{aa}^p\right]^{[k-1]}\mathbf{K}_{Ca}^{[k-1]}\mathbf{F}_{Ra}^{[k-1]}+\mathbf{F}_{Ra}^{[k-1]}\mathbf{K}_{Ca}^{[k-1]}\left[\mathbf{F}_{aa}^p\right]^{[k-1]}-\mathbf{F}_{Ra}^{[k-1]} \tag{19}$$

where k = 1, 2, …, and superscript 'E' denotes the experimental variables. The master DOFs can be chosen in local area, where the substructural flexibility of one or more substructures is extracted. Accordingly, the global flexibility $\left(\overline{\mathbf{F}}_g\right)_{aa}^E$ is obtained by measuring the local area solely.

3. SUBSTRUCTURE BASED MODEL UPDATING

Using the extracted substructural flexibility matrix, the sub-models of one or more substructures can be updated independently. It is necessary to normalize the substructural flexibility matrix calculated from the analytical model and that extracted from experiment to make them comparable in model updating. In the present substructuring method, a projector associated with the mass-normalized mode shapes is constructed to ensure that the substructural flexibility matrix extracted is mass-normalized and is orthogonal to the rigid body modes.

Considering the mass-normalized mode shapes measured in incomplete DOFs, the condensed eigenequation is first formulated according to the IOR method proposed by Xia and Lin (2004)

$$\mathbf{K}_R\mathbf{\Phi}_a = \lambda\mathbf{M}_R\mathbf{\Phi}_a \tag{20}$$

where $\mathbf{K}_R = \mathbf{K}_{aa} - \mathbf{K}_{ab}\mathbf{K}_{bb}^{-1}\mathbf{K}_{ba}$ is the static condensed stiffness matrix, and $\mathbf{M}_R$ is the dynamic condensed mass matrix obtained in an iterative way. Since $\mathbf{M}_R$ is usually unsymmetrical, it needs to be decomposed as $\mathbf{M}_R = \mathbf{M}_1\mathbf{M}_2$, and the condensed projector $\mathbf{P}_R$ is constructed as

$$\mathbf{P}_R = \mathbf{I} - \mathbf{M}_2\mathbf{R}_a\left[\mathbf{M}_1^T\mathbf{R}_a\right]^T \tag{21}$$

It is assumed that the jth substructure is uncertain or damaged with high probability and needs updating. The global structure is measured at the local area corresponding to the jth substructure solely, from which the substructural flexibility of the jth substructure is extracted employing the proposed substructuring approach. Based on the extracted substructural flexibility matrix, the sub-model of the jth substructure is updated independently as follows.

Construct the projector $\mathbf{P}_R^{(j)}$ for the jth substructure. The condensed stiffness matrix $\mathbf{K}_R^{(j)}$, the condensed mass matrix $\mathbf{M}_R^{(j)}$ (Xia and Lin 2004), and the rigid body modes $\mathbf{R}_a^{(j)}$ at the measured points are formed based on the analytical model, and thereafter the projector $\mathbf{P}_R^{(j)}$ is formulated.

Extract the substructural flexibility matrix from the global flexibility matrix $\left(\mathbf{F}_g\right)_{aa}^E$ measured at the area corresponding to the jth substructure. An iterative scheme is proceeded to extract the substructural flexibility matrix $\left(\mathbf{F}_R^{(j)}\right)^E$, following Eq. (19).

Normalize the extracted substructural flexibility matrix. The normalized substructural flexibility matrix is obtained by

$$\mathbf{P}_1^{(j)} = \left(\mathbf{M}_R^{(j)} \backslash \mathbf{M}_1^{(j)}\right)\mathbf{P}_R^{(j)}\mathbf{M}_2^{(j)},\ \mathbf{P}_2^{(j)} = \left[\mathbf{P}_1^{(j)}\right]^T = \mathbf{M}_2^{(j)}\mathbf{P}_R^{(j)}\left(\mathbf{M}_1^{(j)} / \mathbf{M}_R^{(j)}\right),\ \left(\tilde{\mathbf{F}}_R^{(j)}\right)^E = \mathbf{P}_1^{(j)}\left(\mathbf{F}_R^{(j)}\right)^E\mathbf{P}_2^{(j)} \tag{22}$$

where $\mathbf{M}_R^{(j)} = \mathbf{M}_1^{(j)}\mathbf{M}_2^{(j)}$.

Update the analytical sub-model of the jth substructure. The jth substructure is treated as an independent structure and is updated using the conventional global approach. The substructural flexibility matrix $\left(\mathbf{F}_R^{(j)}\right)^A$ corresponding to the measured DOFs is estimated by the analytical model in each iteration and is normalized with $\left(\tilde{\mathbf{F}}_R^{(j)}\right)^A = \mathbf{P}_1^{(j)}\left(\mathbf{F}_R^{(j)}\right)^A\mathbf{P}_2^{(j)}$. The elemental parameters in the jth substructure are adjusted to minimize the difference between the normalized $\left(\tilde{\mathbf{F}}_R^{(j)}\right)^A$ and $\left(\tilde{\mathbf{F}}_R^{(j)}\right)^E$, i.e., minimize $\Delta\mathbf{F} = norm\left(\left(\tilde{\mathbf{F}}_R^{(2)}\right)^E - \left(\tilde{\mathbf{F}}_R^{(2)}\right)^A\right)$.

4. CASE STUDY

This substructuring method is applied to a laboratory tested frame structure as shown in Figure 1 (a). The dimension of the frame structure and the measured points are detailed in Figure 1(b). The global structure is modeled by 45 two-dimensional beam elements and 44 nodes as shown in Figure 1(c), which are separated into three substructures. Figure 1(c) numbers the elements for both the global structure and the independent substructures. The substructural flexibility matrices of the three substructures are extracted from the measurement data in the undamaged states and are used to update the three initial sub-models. The three refined sub-models are subsequently used for damage identification.

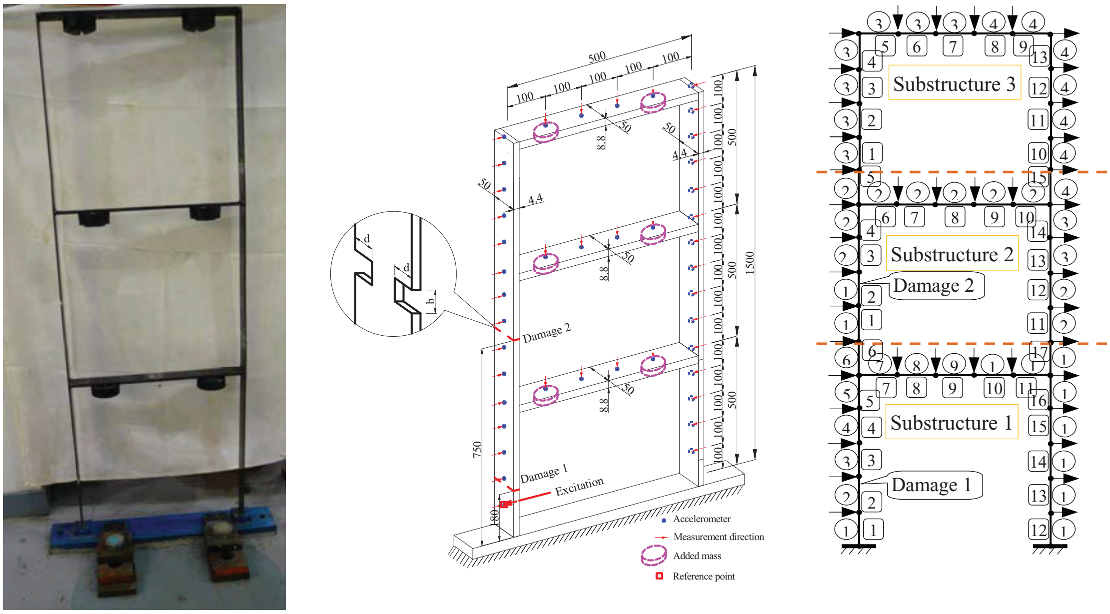

Figure 1: Laboratory tested frame structure; (a):Experimental specimen; (b): Configurations; (c) Analytical model

In the undamaged state, the mass-normalized flexibility matrix is obtained from the measured frequencies and mode shapes as $\mathbf{F}_g^E = \mathbf{\Phi}^E \left(\mathbf{\Lambda}^E\right)^{-1} \left[\mathbf{\Phi}^E\right]^T$ ($\mathbf{\Phi}^E$ and $\mathbf{\Lambda}^E$ are the measured mode shapes and the square of the measured frequencies, respectively). Using the proposed substructuring method, the substructural flexibility of the three substructures are extracted and used as reference to update the three sub-models. Figure 2 reports the stiffness reduction factors (SRF) of the three substructures after updating their respective sub-models according to the procedure described in Section 3.

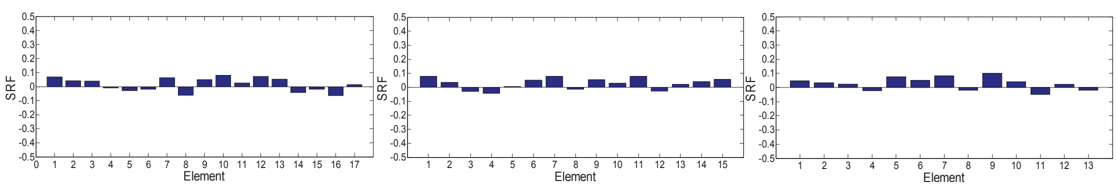

Figure 2: SRF values of the three substructures in the undamaged state; (a) Substructure 1; (b) Substructure 2; (c) Substructure 3.

Afterwards, the three refined sub-models are used for damage identification. In the first damage configuration, the artificial cut is introduced in the first substructure. The 17 elemental parameters in the first substructure are adjusted, whereas the sub-models of the second and third substructures remain unchanged. In the experiment, only the first substructure was measured to form the flexibility matrix $\left(\mathbf{F}_g\right)_{aa}^E$. The substructural flexibility matrix of the first substructure is extracted from the measured flexibility matrix $\left(\mathbf{F}_g\right)_{aa}^E$ and used as reference to adjust the elemental parameters in the first substructure. Figure 3 shows the SRF values of the 17 elemental parameters after updating. It is observed that the SRF of Element 2 is -23%, and small SRF values ranging from 0 to -10% exist in some other elements.

In the second damage configuration, two artificial cuts are located in different substructures. The frequencies and mode shapes measured in the first and second substructures are used to form the global flexibility matrix $\left(\mathbf{F}_g\right)_{aa}^E$. The normalized substructural flexibility matrices of the first substructure $\left(\tilde{\mathbf{F}}_R^{(1)}\right)^E$ and the second substructure $\left(\tilde{\mathbf{F}}_R^{(2)}\right)^E$ are extracted from $\left(\mathbf{F}_g\right)_{aa}^E$ simultaneously. The analytical sub-models of the first and second substructures are subsequently updated to recover $\left(\tilde{\mathbf{F}}_R^{(1)}\right)^E$ and $\left(\tilde{\mathbf{F}}_R^{(2)}\right)^E$, respectively. Figure 4 shows that after updating, the SRF value of Element 2 in the first substructure is about -20% and the SRF value of Element 2 in the second substructure (Element 19 of the global structure) is -25%.

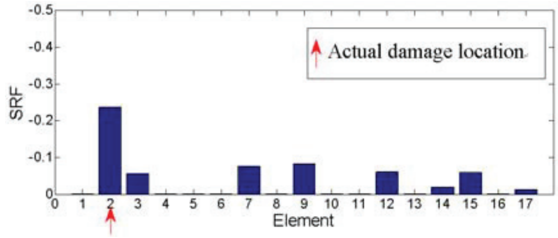

Figure 3: SRF values of the first damage configuration (first substructure).

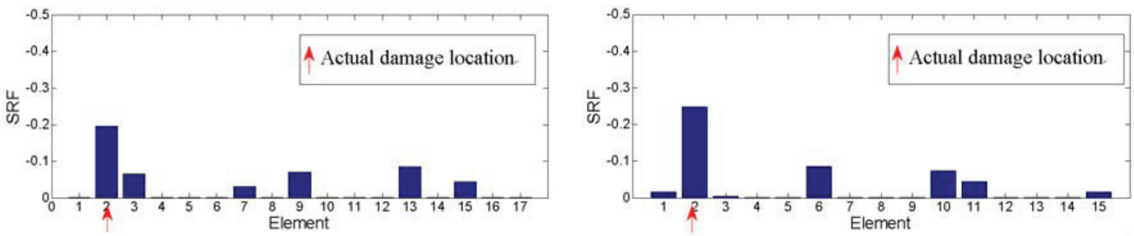

(a) First substructure (b) Second substructure

Figure 4: SRF values of the second damage configuration; (a) First substructure; (b) Second substructure

For comparison, the frame is updated using the traditional global method based on the same measured modal data. Likewise, the difference in the flexibility matrices of the analytical model and the experimental measurements is minimized to adjust the 45 elemental parameters simultaneously. The initial model is first updated using the modal data in the undamaged state. The SRF values of the elemental parameters after updating are shown in Figure 5(a). The refined model is subsequently used for damage identification. The SRF values from the two damage configurations are illustrated in Figure 5(b) and Figure 5(c), respectively. Element 2 is observed to have a clearly negative SRF value of about -25% in both damage configurations. The SRF value of Element 19 is about -30% in the second damage configuration. These observations are consistent with those made for the substructuring based model updating methods described earlier (Figure 3 and Figure 4).

This laboratory tested frame structure has been analyzed using the proposed substructuring based model updating method and the traditional global-based method with the same set of experimental data. Both of the methods can successfully locate artificial cuts and obtain similar results on reductions in elemental stiffness. This demonstrates that the substructuring method proposed in this paper is effective in model updating and damage identification.

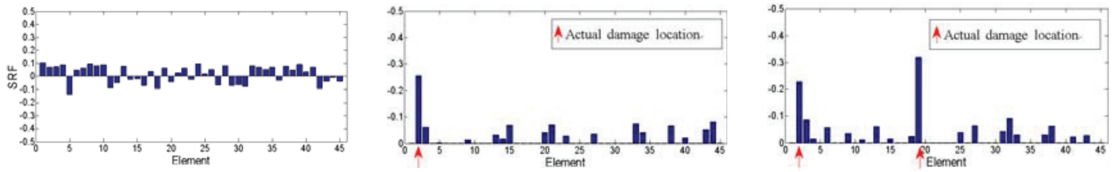

Figure 5: SRF values using the conventional global method; (a) Undamaged state; (b) First damage configuration; (c) Second damage configuration

5. CONCLUSION

This paper proposed a substructuring method to extract the substructural flexibility matrices from the global flexibility matrix of a structure. During the experiment, only the local area corresponding to the interested substructure is required to be measured. Thereafter the sub-model of particular substructure is updated independently to match the extracted substructural flexibility matrix, using the conventional global-based model updating method. As only a focused substructure is adjusted in model updating, the proposed substructuring method reduces the size of the analytical model involved and decrease the uncertain parameters, thus benefiting the convergence of the optimization process. Application to a laboratory-tested three-storey portal frame structure demonstrates that the proposed substructuring based model updating method can locate the artificial damage successfully and the identified stiffness parameter changes are similar to those obtained by the global based model updating method. This substructuring based model updating method is effective to be used in model updating and damage identification.

Reference

[1] Alvin KF, Park KC (1999). Extraction of substructural flexibility from global frequencies and mode shapes. AIAA Journal. 37(11), pp.1444-1451.

[2] Brownjohn JMW (2007). Structural health monitoring of civil infrastructure. Philosophical Transactions of the Royal Society A: Mathematical, Physical & Engineering Sciences. 365(2), pp.589-622.

[3] Duan YF, Xu YL, Fei QG, Wong KY, Chan KWY, and Ni YQ (2006). Full 3D finite element model for criticality analysis of Tsing Ma Bridge. Proceedings of International Conference on Bridge Engineering, Hong Kong.

[4] Koh DG, Hong B, Liaw DY (2003). Substructural and progressive structural identification method, Engineering Structures. 25(2003), pp.1551-1563.

[5] Weng S, Xia Y, Xu YL, Zhou XQ, Zhu HP (2009). Improved substructuring method for eigensolutions of large-scale structures. Journal of Sound and Vibration. 323(3-5), pp.718-36.

[6] Xia Y, Hao H, Deeks AJ, and Zhu XQ (2008). Condition Assessment of Shear Connectors in Slab-Girder Bridges via Vibration Measurements. Journal of Bridge Engineering. 13(1), pp.43-54.

[7] Xia Y, Weng S, Xu YL, and Zhu HP (2010). Calculation of Eigenvalue and Eigenvector Derivatives with the Improved Kron's Substructuring Method. Structural Engineering and Mechanics. 36 (1), pp.37-55.

[8] Klerk D, Rixen DJ, Voormeeren SN (2008).General Framework for Dynamic Substructuring: History, Review, and Classification of Techniques. AIAA Journal. 46, pp.1169-1181.

[9] Lallemand B, Level P, Duveau H, and Mahieux B (1999). Eigensolutions sensitivity analysis using a sub-structuring method. Computers and Structures. 71(3), pp.257-265.